

ESTIMATION OF GLT BEAM STIFFNESS BASED ON HOMOGENIZED BOARD MECHANICAL PROPERTIES AND COMPOSITE BEAM THEORY

GIUSEPPE BALDUZZI¹, GEORG KANDLER² AND JOSEF FÜSSL¹

¹ Institute for Mechanics of Materials and Structures, Vienna University of Technology
Karlsplatz 13/202, 1040 Vienna, Austria
giuseppe.balduzzi@tuwien.ac.at josef.fuessl@tuwien.ac.at, <http://www.imws.tuwien.ac.at>

² Dynardo Austria GmbH
Wagenseilgasse 14, 1120 Vienna, Austria
georg.kandler@dynardo.at, <http://www.dynardo.at>

Key words: glued laminated timber, first order shear deformation theory, axial stiffness, bending stiffness, dynamic test, four point bending test

Abstract. This paper aims at estimating the stiffness of Glued Laminate Timber (GLT) beams on the basis of an accurate analysis of the board's mechanical properties and a simple composite beam theory. Modern grading technologies, like laser scanning, have the capability to accurately detect grain orientation on the surface of timber boards, allowing for an accurate analysis of local mechanical properties. Conversely, this information is only partially exploited in the estimation of strength and stiffness of GLT structural elements since, also nowadays, the mechanical properties of GLT beams are evaluated only on the basis of boards grading, leading to extremely cautious but also coarse estimations. A recent paper exploits information on wood's mechanical properties and high resolution data on grain orientation in order to estimate GLT beam stiffness obtaining promising results. Unfortunately, the approach needs highly refined 2D Finite Element (FE) analysis resulting quite expensive from the computational point of view. Aiming mainly at reducing the computational cost, this paper exploits high resolution information for the estimation of homogenized mechanical properties of boards. Thereafter, it uses the so called composite beam theory for the direct estimation of the GLT beam stiffness. The comparison with experimental data highlights that the proposed approach provides estimations with an accuracy similar to 2D FE analysis, but, since it is significantly cheaper, it turns out to be more convenient. Finally, the simplicity of the beam model allows for an easier understanding of relations between input and output, facilitating a more rigorous interpretation of experimental data.

1 INTRODUCTION

Timber is an excellent building material: it comes from a renewable resource, exhibits a very good strength vs weight ratio combined with good insulation properties, and its

life cycle assessment is considered to be very positive. As a consequence, its usage is worldwide increasing and the technologies used in wood industry are continuously evolving in order to increase the efficiency of production processes and the performance of wooden products. One big challenge, however, is that wood is a naturally grown material and its mechanical properties are subjected to high variability. As a consequence, to meet reliability, safety, and functionality requirements of structural elements, national and international standards define very conservative processes in raw material selection and high safety coefficients for both ultimate and serviceability limit state analysis (UNI EN 1408, 2011; EN 1995, 2004). Obviously, this translates into a low exploitation of the real material potential. Thus, the development of new and more accurate grading strategies as well as the exploitation of newly available technologies are strongly in the focus of wood research (Pettersson, 2010; Olsson et al., 2012). In practice, for example, this trend leads industries to progressively abandon manual grading of boards which is replaced by automatic grading machines in Glued Laminated Timber (GLT) beam production lines.

Within this complex and evolving context, several efforts are contributing to the definition of new procedures for an effective estimation of the GLT beams' mechanical properties. As an example, Olsson et al. (2013) proposed a new and accurate grading method for timber boards. Specifically, they detect the grain angles on board's surfaces using a high resolution laser scanner device. Thereafter, they use this information for computing local Modulus of Elasticity (MOE) and, through simple homogenization technique and suitable calibration of parameters, cross-sectional stiffnesses. Finally, they identify the minimal cross-section stiffness as a property highly correlated with boards' strength. Aiming at evaluating the effectiveness of the proposed procedure in predicting timber boards' mechanical properties, Olsson et al. (2013) compare the proposed method with several others existing in literature and extensively used in wood industry. The analysis of 105 boards of Norway spruce indicates that the proposed procedure gives the possibility to significantly enhance the effectiveness of boards' grading.

According to these results, Kandler et al. (2015) exploited the laser scanner technology in order to predict GLT beam stiffnesses. Specifically, they evaluate the clear wood mechanical properties according to an enhanced MicroMechanical Model (MMM) (Hofstetter et al., 2005) and, on the basis of high resolution information on grain angle, estimate the local axial stiffness of 350 boards from grading classes LS15 and LS22. The comparison with dynamical tests on boards reveals a good accuracy of the proposed procedure with coefficient of determination $R^2 > 0.85$. Thereafter, they assemble boards in 50 GLT beams (including 5 different configurations) tracking the lamellas throughout the production process. Finally, they use information on stiffness distribution in a highly refined 2D Finite Element (FE) model and run linear analysis in order to estimate the stiffness of assembled GLT beams. Comparison with four point bending test highlights that the proposed procedure turns out to be accurate, with coefficient of determination $R^2 > 0.85$. Unfortunately, despite the high accuracy obtained by the so far introduced procedure, the 2D FE model needs up to $\sim 160\,000$ Degrees Of Freedom (DOFs), resulting therefore too expensive and slow, especially if compared with the speed of machinery in modern GLT production plants.

This paper proposes a modification of the procedure proposed by Kandler et al. (2015). In particular, aiming at avoiding the bottle-neck of highly refined 2D FE analysis, this paper applies the so called theory of composite beams for the recovery of cross-section stress distributions. Subsequently, this information is used for an effective and energetically consistent evaluation of axial, bending, and shear stiffnesses.

On the one hand, the theory of composite beams is based on Timoshenko kinematics (i.e., it assumes that the cross-section is rigid and can rotate with respect to the beam centerline), but, given the internal forces and the beam geometry, provides a more accurate reconstruction of the stress distributions within the cross-section (Bauchau and Craig, 2009, Chapter 5). As a significant example, it is worth mentioning that Frese and Blaß (2012) exploit the composite beam theory for the recovery of stress distribution within a computer model for the estimation of both stiffness and strength of asymmetrically combined GLT beams.

The simplicity of both the theory of composite beams and the procedure for stiffness calculation has the following three main advantages:

1. the drastic reduction of the computational cost,
2. the capability, starting from information on local boards mechanical properties, to directly provide parameters useful for practitioners and consistent with models (e.g., Timoshenko beams and FE) usually employed in structural analysis, and
3. the possibility to easily recognize the influence of several parameters on the GLT beam stiffness.

This paper aims at investigating the accuracy and effectiveness of such an approach for the estimation of GLT beams. Accordingly, the paper uses data on boards MOE reported in (Kandler et al., 2015) as input for the calculation of the beam stiffness and thereafter uses the results of tests on assembled GLT beams in order to validate the proposed modeling approach. The paper is structured as follows: Section 2 resumes the procedure for the determination of the board’s stiffness, Section 3 provides formulas for the estimation of beam stiffness, Section 4 analyzes the obtained numerical results, and Section 5 discusses final remarks and delineate future research.

2 SYNOPSIS OF THE PROCEDURE FOR THE DETERMINATION OF THE BOARD’S STIFFNESS

This work uses the results obtained in the study of Kandler et al. (2015). The procedure presented therein includes (a) the computation of the clear wood stiffness tensor using MMM and (b) the homogenisation over each cross section to obtain a so-called stiffness profile $E_{\text{board}}(x)$. MMM takes clear wood density, moisture content, microfibril angle and species specific properties into account (Hofstetter et al., 2005). While the clear wood properties are assumed constant within each board, the fibre angle course varies strongly, particularly in the vicinity of knots (Phillips et al., 1981). Therefore, Kandler et al made use of fibre angle measurements obtained by employing a tracheid effect-based laser

scanning device (Pettersson, 2010). The measurements are obtained on a grid of approx. 1 mm in longitudinal direction and 4 mm in lateral direction of the board. In each measurement point, the previously obtained clear wood stiffness tensor is transformed according to the corresponding fibre angle value. Thereafter, for each cross section, the mean value of the stiffness tensor component in x -direction is computed, resulting in a stiffness profile as shown in Figure 1b.

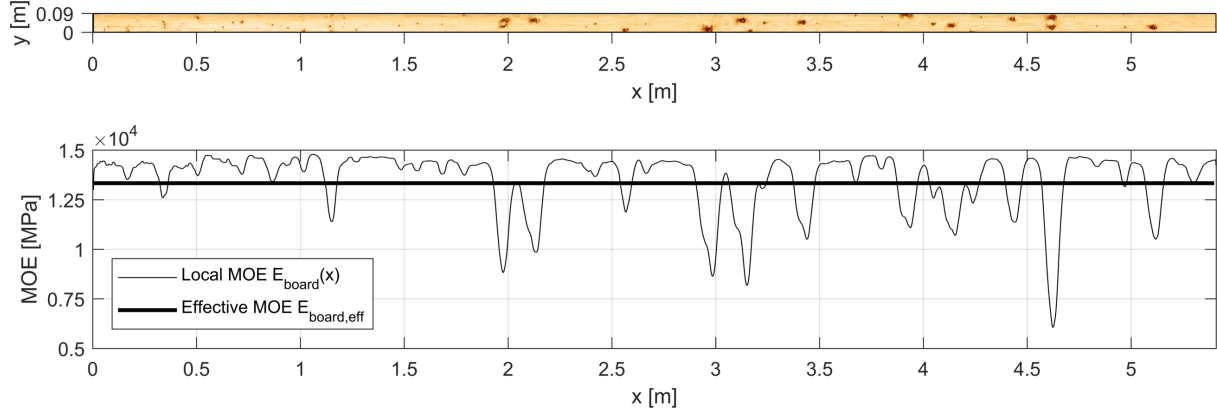


Figure 1: (a) Typical wooden board and (b) resulting stiffness profile as well as the effective stiffness value.

In contrast to the full stiffness profile model, in this work the input information is reduced to a constant, homogenised stiffness value $E_{\text{board,eff}}$ for each lamella. For the homogenised stiffness, the model analogy of strings in series is employed, i. e. an effective longitudinal stiffness value $E_{\text{board,eff}}$ for each board is computed according to

$$E_{\text{board,eff}} = \frac{L}{\int_{x=0}^L \frac{1}{E_{\text{board}}(x)} dx}, \quad (1)$$

where $E_{\text{board}}(x)$ is the stiffness profile and L is the length of the board. On average, the homogenised stiffness value is 12.4% and 7.3% lower than the maximum stiffness profile value (which corresponds to the clear wood stiffness value), for the two grading classes LS15 and LS22, respectively. The only factor responsible for this difference is the fibre angle distribution within each board. Since for the higher grading class LS22 less knots and less fibre deviations are observed, it is also reasonable that the difference between maximum stiffness value and homogenised stiffness value is smaller than for the lower grading class.

3 STIFFNESS ESTIMATIONS BASED ON COMPOSITE BEAM THEORY

This section provides the formulas used for the cross-section stiffness estimation. Specifically, according to the Timoshenko kinematics, the composite beam theory assumes that the cross-section is rigid and can rotate around the cross-section neutral axis, parallel to

the z axis. As a consequence, axial strain $\varepsilon_{xx}(y)$ has a linear distribution with respect to the thickness coordinate y , as illustrated in Figure 2 (c). Thereafter, considering the layered non-homogeneous cross-section depicted in Figure 2 (a) and the piecewise constant distribution of axial MOE $E(y)$ depicted in Figure 2 (b), the axial stress turns out to be piecewise linear with respect to y i.e., $\sigma_{xx}(y) = E(y) \cdot \varepsilon_{xx}(y)$ as illustrated in Figure 2 (d).

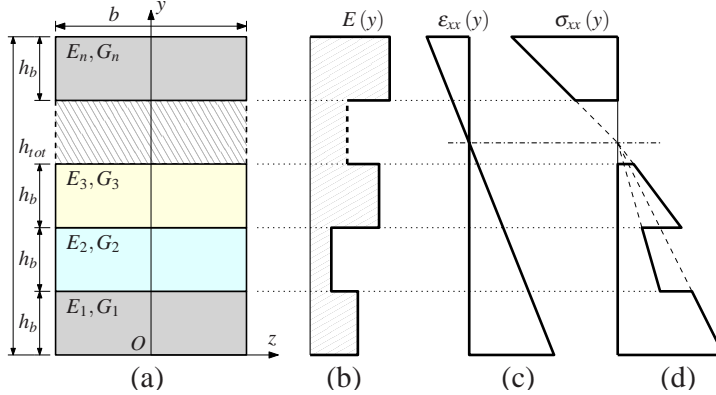


Figure 2: GLT beam cross-section geometry (a), MOE $E(y)$ (b), axial strain $\varepsilon_{xx}(y)$ (c), and axial stress $\sigma_{xx}(y)$ (d) distributions within the cross-section. Adopted notation: n number of layer constituting the beam, h_b board's thickness, b beam depth, board's mechanical properties: E_i and G_i longitudinal MOE and shear modulus, respectively.

The GLT beam axial stiffness is defined as

$$EA^* = b \int_0^{h_{tot}} E(y) dy \quad (2)$$

the y coordinate of the neutral axis of the cross-section subjected to a pure bending moment reads

$$c^* = \frac{b \int_0^{h_{tot}} E(y) y dy}{EA^*} \quad (3)$$

and, finally, the GLT beam bending stiffness reads

$$EI^* = b \int_0^{h_{tot}} E(y) (y - c^*)^2 dy \quad (4)$$

For convenience, we introduce the equivalent MOE of the beam that could be defined according to the axial stiffness

$$E^{axial} = \frac{EA^*}{bh_{tot}} \quad (5)$$

or according to the bending stiffness

$$E^{bend} = EI^* \frac{12}{bh_{tot}^3} \quad (6)$$

It is obvious that, considering composite beams, Equations (5) and (6) provide different estimations of the beam's MOE. At least, estimation provided by Equation (6) is sensitive to the board's layout whereas the estimation provided by Equation (5) is not influenced by any permutation of the board's order. Considering the great dispersion (i.e., the considerable standard deviation) of the board's MOE (see e.g., Kandler et al., 2015, Table 3), it is reasonable to expect some difference between the two herein proposed estimations. Conversely, the timber engineering practice does not distinguish axial and bending MOEs (Porteous and Kermani, 2013; BS EN 1194, 1999).

4 NUMERICAL RESULTS

This section compares numerical and experimental results regarding the evaluation of the bending (Subsection 4.1) and the axial MOE (Subsection 4.2).

4.1 Bending MOE

This section compares the bending MOE estimations provided by Equation (6) and the ones based on four point bending tests. Kandler et al. (2015) provide the board's longitudinal stiffness on the basis of the results of axial dynamical tests and on the basis of MMM and grain angle. Consistently, the estimation of the bending GLT beam MOE will be indicated as $E_{num,dyn}^{bend}$ or $E_{num,MMM}^{bend}$, according to the source of board's data employed for the calculation. The estimations based on the four point bending tests, obtained according to the procedure detailed by Kandler et al. (2015) and indicated in the following as E_{exp}^{bend} , are herein considered as reference values.

In Figure 3 the bending MOE values $E_{num,dyn}^{bend}$ evaluated on the basis of board's dynamic tests are plotted against the experimental results of the four point bending tests E_{exp}^{bend} . In Table 1 the relative statistics are reported.

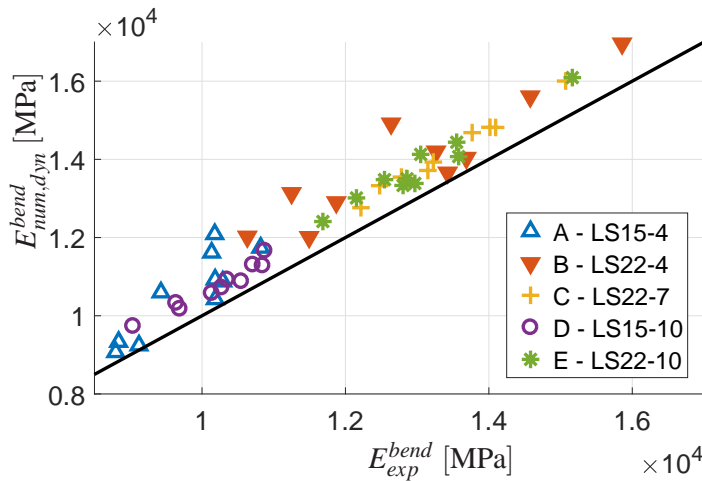


Figure 3: Comparison of the GLT beam bending MOE $E_{num,dyn}^{bend}$ evaluated on the basis of board's dynamic tests with the experimental results of the four point bending tests E_{exp}^{bend} .

	A	B	C	D	E	All
R^2	0.766	0.823	0.986	0.942	0.951	0.951
\bar{e}	0.080	0.086	0.056	0.054	0.058	0.067
s	0.057	0.056	0.009	0.015	0.017	0.038

Table 1: Coefficient of determination R^2 for the GLT beam bending MOE evaluated on the basis of board's dynamic tests $E_{num,dyn}^{bend}$ and the experimental results of the four point bending tests E_{exp}^{bend} , estimation of the mean value \bar{e} and the standard deviation s of the normalized error.

For the prediction of the bending MOE $E_{num,dyn}^{bend}$ the coefficient of determination R^2 ranges from 0.77 to 0.99 considering separately each type of beam whereas the coefficient of determination R^2 for all the types is equal to 0.95. Conversely, looking at the normalized error \bar{e} , it is possible to notice that the bending MOE $E_{num,dyn}^{bend}$ tend to overestimate the experimental data E_{exp}^{bend} , with an error ranging from 5% to 9%. Finally, the standard deviation of the normalized error s ranges from 1.5e-2 to 5.7e-2.

In Figure 4 the bending MOE values $E_{num,MMM}^{bend}$ evaluated on the basis of MMM and grain angle are plotted against the experimental results of the four point bending tests E_{exp}^{bend} . In Table 2 the relative statistics are reported.

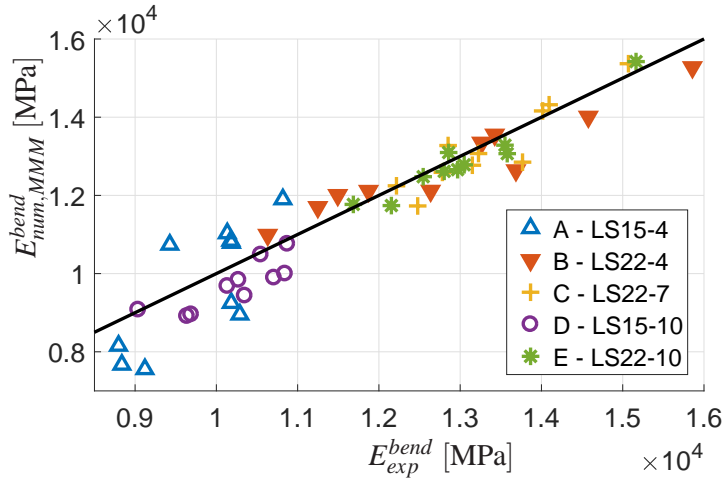


Figure 4: Comparison of the GLT beam bending MOE $E_{num,MMM}^{bend}$ evaluated on the basis of MMM and grain angle with the experimental results of the four point bending tests E_{exp}^{bend} .

	A	B	C	D	E	All
R^2	0.546	0.919	0.847	0.693	0.936	0.903
\bar{e}	-0.015	-0.004	-0.010	-0.049	-0.011	-0.017
s	0.116	0.042	0.033	0.035	0.020	0.059

Table 2: Coefficient of determination R^2 for the GLT beam bending MOE evaluated on the basis of MMM and grain angle $E_{num,MMM}^{bend}$ and the experimental results of the four point bending tests E_{exp}^{bend} , estimation of the mean value \bar{e} and the standard deviation s of the normalized error.

For the prediction of the bending MOE $E_{num,MMM}^{bend}$ the coefficient of determination R^2 ranges from 0.55 to 0.94 considering separately each type of beam whereas the coefficient of determination R^2 for all the types is equal to 0.9. Furthermore, $E_{num,MMM}^{bend}$ evaluated via the composite beam theory tends to underestimate the experimental data with a maximal error of 5% and a mean value smaller than 2%. Finally, the standard deviation of the normalized error s ranges from 2.0e-2 to 11.6e-2.

Comparing this results with the ones reported in (Kandler et al., 2015, Table 5), it is possible to appreciate how the simplified estimation herein proposed leads to increase the coefficient of determination considering both all the samples together and each type separately. Furthermore, it is possible to notice that the simplified approach generally reduces or do not affect the magnitude of both the normalized error and the standard deviation for each beam type considered separately (with the exception of types D). Conversely, analyzing all the samples together, it is possible to notice how the simplified approach tends to underestimate whereas 2D FE tends to overestimate experimental data, despite the magnitude of error and standard deviation are similar.

4.2 Axial MOE

This section compares the axial MOE estimations provided by Equation (5) and the ones based on dynamic tests. The estimation of the axial GLT beam MOE will be indicated as $E_{num,dyn}^{axial}$ or $E_{num,MMM}^{axial}$, according to the source of the board's data employed for the calculation. Conversely, the estimations based on the dynamic tests on beams, obtained according to the procedure detailed by Kandler et al. (2015) and indicated in the following as E_{exp}^{axial} , are herein considered as reference values.

In Figure 5 the bending MOE values $E_{num,dyn}^{axial}$ evaluated on the basis of board's dynamic tests are plotted against the experimental results of the beam's dynamic tests E_{exp}^{axial} . In

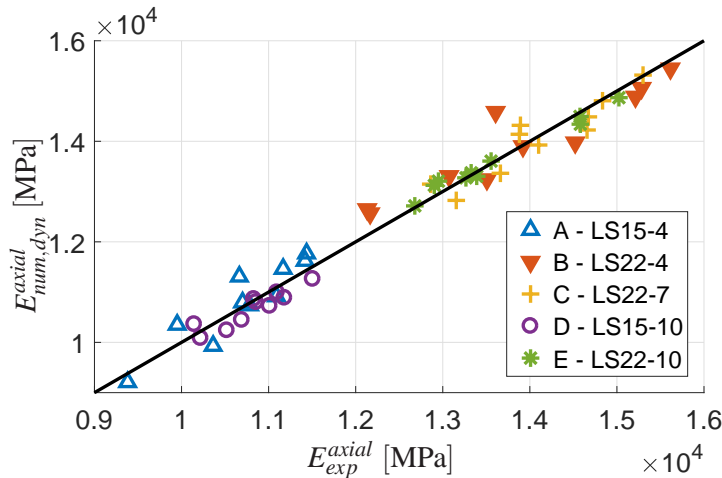


Figure 5: Comparison of the GLT beam axial MOE $E_{num,dyn}^{axial}$ evaluated on the basis of board's dynamic tests with the experimental results of the beam's dynamic tests E_{exp}^{axial} .

Table 3 the relative statistics are reported.

	A	B	C	D	E	All
R^2	0.850	0.876	0.862	0.848	0.981	0.970
\bar{e}	0.010	0.006	-0.003	-0.013	0.001	0.000
s	0.031	0.034	0.021	0.016	0.011	0.025

Table 3: Coefficient of determination R^2 for the GLT beam axial MOE evaluated on the basis of board’s dynamic tests $E_{num,dyn}^{axial}$ and the experimental results of the beam’s dynamic tests E_{exp}^{axial} , estimation of the mean value \bar{e} and the standard deviation s of the normalized error.

For the prediction of the axial MOE $E_{num,dyn}^{axial}$ the coefficient of determination R^2 ranges from 0.85 to 0.98 considering separately each type of beam whereas the coefficient of determination R^2 for all the types is equal to 0.97. Furthermore, looking at the normalized error \bar{e} , it is possible to notice that the axial MOE $E_{num,dyn}^{axial}$ is a good estimation of the experimental data E_{exp}^{axial} , with an error magnitude always smaller or equal than 1% for all the types, with the exception of type D. Finally, the standard deviation of the normalized error s ranges from 1.1e-2 to 3.4e-2.

Comparing this results with the ones reported in (Kandler et al., 2015, Table 4), it is possible to appreciate how the herein proposed simplified estimation leads to increase significantly the coefficient of determination, especially when each type is considered separately. Furthermore, it is possible to notice a moderate reduction of the normalized error (excluding types A and E) whereas the standard deviation of the simplified approach is approximatively the half of the one obtained using enhanced FE. Maybe, accounting for the stiffness variations along the boards introduces some noise in the modeling procedure proposed in (Kandler et al., 2015), leading to the lower correlation so far highlighted. Furthermore, since both the input data for the model and the reference values E_{exp}^{axial} are obtained using the same experimental procedure, both are affected by the same systematic errors, leading to the highest coefficients of determination and the lowest normalized error \bar{e} and standard deviation s .

In Figure 6 the axial MOE values $E_{num,MMM}^{axial}$ evaluated on the basis of MMM and grain angle are plotted against the experimental results of the beam’s dynamic tests E_{exp}^{axial} . In Table 4 the relative statistics are reported.

	A	B	C	D	E	All
R^2	0.578	0.867	0.519	0.384	0.935	0.892
\bar{e}	-0.078	-0.083	-0.066	-0.112	-0.065	-0.081
s	0.094	0.031	0.042	0.037	0.015	0.052

Table 4: Coefficient of determination R^2 for the GLT beam axial MOE evaluated on the basis of MMM and grain angle $E_{num,MMM}^{axial}$ and the experimental results of the beam’s dynamic tests E_{exp}^{axial} , estimation of the mean value \bar{e} and the standard deviation s of the normalized error.

For the prediction of the axial MOE $E_{num,MMM}^{axial}$ the coefficient of determination R^2 ranges from 0.38 to 0.94 considering separately each type of beam whereas the coefficient of determination R^2 for all the types is equal to 0.89. Furthermore, looking at the normalized error, it is possible to notice that the axial MOE $E_{num,MMM}^{axial}$ tends to underestimate the

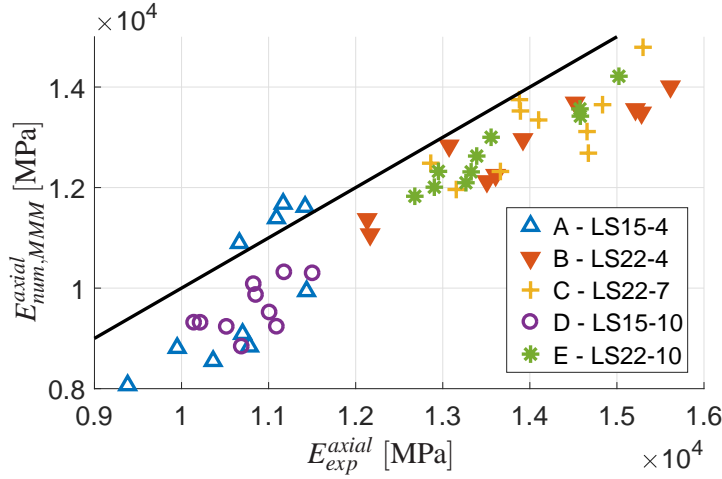


Figure 6: Comparison of the GLT beam axial MOE $E_{num,MMM}^{axial}$ evaluated on the basis of MMM and grain angle with the experimental results of the beam’s dynamic tests E_{exp}^{axial} .

experimental data E_{exp}^{axial} , with an error magnitude ranging from 6% to 11%. Finally, the standard deviation of the normalized error ranges from 1.5e-2 to 9.5e-2, resulting similar to one obtained for bending MOE.

5 CONCLUSIONS

This paper considers a simplified approach for the evaluation of the GLT beam stiffness based on an accurate analysis of the board mechanical properties and the theory of composite beams.

The comparison of the results obtained with the herein proposed simplified method, refined 2D FE analysis, and experimental tests allows to conclude that the simplified method provides reasonable estimations in most of cases. In particular the following main conclusions can be drawn:

1. The accuracy of the stiffness estimations proposed in Section 3 are similar or even slightly better than refined 2D FE analysis proposed in (Kandler et al., 2015). It is reasonable to suppose that highly refined data on stiffness distributions are affected by some error. Maybe, the FE analysis propagates this error whereas the simplified formulas, using averaged values, mitigate the effects of noise on board’s data.
2. Results obtained on the basis of board’s dynamic tests have generally an higher coefficient of determination and a lower standard deviation of the normalized error if compared with the results obtained from MMM and grain angle. This trend is expected since dynamic testing directly provides averaged information for the whole board, avoiding therefore error propagation coming from elaboration of local information on grain angle and error source represented by the estimation of MMM parameters.
3. Distinction of axial and bending MOE allows for a better fitting of both data coming

from dynamic and four point bending tests on beams, indicating that the adoption of a unique mechanical parameter E in order to identify the beam stiffness may introduce undesirable errors.

On the one hand, since the simplified approach turns out to be significantly cheaper than the considered 2D FE, it maybe represents a better approach for the estimation of the GLT beam bending MOE. On the other hand, the composite beam theory can not provide any information on local stress distributions. Therefore, it is expected to be a coarse instrument for the estimation of GLT beam strength.

Future research includes the consideration of more refined beam theories in order to model the effects of knot distributions.

ACKNOWLEDGMENTS

This work was funded by the Austrian Science Found (FWF) trough the Project # M 2009-N32.

References

- Bauchau, O. and J. Craig (2009). *Structural Analysis With Applications to Aerospace Structures*, Volume 163 of *Solid mechanics and its applications*. Springer Netherlands.
- BS EN 1194 (1999, September). Timber structures. glued laminated timber. strength classes and determination of characteristic values.
- EN 1995 (2004, April). Eurocode 5: Design of timber structures.
- Frese, M. and H. J. Blaß (2012). Asymmetrically combined glulam simplified verification of the bending strength. In *CIB-W18/45-12-1 International Council for Reserach and Innovation in Builfing and Construction, Working Commission W18 – timber structures – Meeting fortyfive Växjö Sweden August 2012*.
- Hofstetter, K., C. Hellmich, and J. Eberhardsteiner (2005). Development and experimental validation of a continuum micromechanics model for the elasticity of wood. *European Journal of Mechanics-A/Solids* 24(6), 1030–1053.
- Kandler, G., J. Füssl, E. Serrano, and J. Eberhardsteiner (2015). Effective stiffness prediction of glt beams based on stiffness distributions of individual lamellas. *Wood Science and Technology* 49(6), 1101–1121.
- Olsson, A., J. Oscarsson, M. Johansson, and B. Källsner (2012). Prediction of timber bending strength on basis of bending stiffness and material homogeneity assessed from dynamic excitation. *Wood science and technology* 46(4), 667–683.
- Olsson, A., J. Oscarsson, E. Serrano, B. Källsner, M. Johansson, and B. Enquist (2013). Prediction of timber bending strenght and in-member cross-sectional stiffness variation on the basis of local wood fibre orientation. *European Journal of Wood Product* 71, 319–333.

Petersson, H. (2010). Use of optical and laser scanning techniques as tools for obtaining improved fe-input data for strength and shape stability analysis of wood and timber. In *IV European conference on computational mechanics, Paris, France*.

Phillips, G., J. Bodig, and J. Goodman (1981). Flow-grain analogy. *Wood Science* 14(2), 55–64.

Porteous, J. and A. Kermani (2013). *Structural Timber Design to Eurocode 5*. Wiley.

UNI EN 1408 (2011). Timber structures - structural timber with rectangular cross section classified according to the resistance.